International Journal of Materials and Chemistry 2015, 5(3): 49-53
DOI: 10.5923/j.ijmc.20150503.01

Fabrication of Regenerated Cellulose-based Resonant Magnetic Field Sensors based on MEMS Technology

Nargis A. Chowdhury[1,*], Maximiano V. Ramos[2], Ahmed Al-Jumaily[1], John Robertson[3]

[1]Institute of Biomedical Technologies, Auckland University of Technology, Auckland, New Zealand
[2]School of Engineering, Auckland University of Technology, Auckland, New Zealand
[3]School of Applied Sciences, Auckland University of Technology, Auckland, New Zealand

Abstract This study investigates the performance of magnetic field micro-sensors consisting of regenerated cellulose/ functionalized carbon nanofibers/ polypyrrole (RC/FCNF/PPy coated) and RC/FCNF/PPy (blend) with different preparation processes in terms of electrical conductivity, bending displacement, and electrical power consumption. Optical detection technique is used for measuring the deflections of the film under an external magnetic field parallel to the length of the film. We observed that the deflection of the films is increased, when alternating current is applied with a frequency equal to the bending resonant frequency of the film. We also observed that sensors coated by polypyrrole doped with anthraquinone-2-sulfonic acid sodium salt monohydrate showed improved electrical conductivity compared to that of using perchlorate ion as the dopant. This is due to the preparation process and the effect of dopants which play an important role in improving the properties of the regenerated cellulose-based ionic electro-active sensors. The RC/FCNF /PPy (coated) sensors consumed higher electrical power compared to the RC/FCNF /PPy (blend) sensors due to their higher electrical conductivity values.

Keywords Bending displacement, Electrical conductivity, Magnetic field sensors, Sulfonic acid dopants

1. Introduction

Microelectromechanical systems (MEMS) technology not only combines magnetic field sensors with electronic components but also presents important advantages such as small size, light weight, minimum power consumption, low cost, and better sensitivity. The existing sensors are experiencing some challenges because of their complex fabrication of the magnetic core and the coils [1], as well as high mass and power consumption. Any reduction of their mass and power results in their low sensitivity and stability [2]. They can be operated up to 100 kHz and have a size on the order of several millimeters, and a power consumption around 100 mW. Miniaturization of the coils and the integration of the magnetic core [3] are still challenging. The existing sensors fabricated from regenerated cellulose are experiencing some challenges because of their little displacement output at ambient humidity, small force output and frequency [4] and the performance degrades with time [5]. To resolve this problem, functionalized multi-walled carbon nanotubes (F-MWNTs) blended cellulose electro-active paper (EAPap) sensors were developed with improved actuation force but the power consumption was increased. This might be due to the increased electrical conductivity caused by the high mobility of Cl^- ions and weight percent of F-MWNTs in cellulose matrix [6]. Recently, MEMS technology has been exploited as a candidate for the development of sensors. It can integrate mechanical and electronic components on a substrate. Several resonant magnetic field sensors based on MEMS technology have been developed by some research groups [7]. These sensors are compact and smaller (micrometers sized) than fluxgate, Superconducting Quantum Interference Device (SQUIDs), and optical fiber sensors. Therefore, they can be placed closer to low-magnetic field sources for increasing their output signal. In addition, they are lighter, faster and cheaper than their macroscopic counterparts [7]. These sensors use resonant structures that exploit the Lorentz force principle for detecting magnetic fields. Generally, they measure the displacement of resonant structures exposed to external magnetic fields through optical sensing technique [7].

In this study, two sensors were developed with different preparation processes (blending or coating of polypyrrole) to improve electrical conductivity. In addition, to increase the deflection of the film alternating current is applied with one frequency equal to the bending resonant frequency of the film. The main advantages of using carbon nanofibers are that the material can be manufactured in large scale, can be functionalized easily, smaller in size than multi-walled carbon nanotubes, and incorporating the functionalized

* Corresponding author:
nargis.afroj@aut.ac.nz (Nargis A. Chowdhury)
Published online at http://journal.sapub.org/ijmc

carbon nanofibers into polymers is easier. In addition, the known toxicity of the functionalized carbon nanofibers is significantly lower than the toxicity of functionalized carbon nanotubes [8].

2. Matrices Synthesis

2.1. Materials

The material used in this research:

Dimethylacetamide (DMAC) (Anhydrous 99.8%), 2-propanol, lithium chloride, cotton linter (DPW 4580), carbon nanofibers (CNFs), pyrrole, anthraquinone-2-sulfonic acid sodium salt monohydrate, 5-sulfosalicylic acid dihydrate, and ferric chloride hexahydrate were purchased from Sigma Aldrich, USA. All the chemicals were used as received except pyrrole. Freshly prepared pyrrole was used during polypyrrole synthesis.

2.2. Functionalization of Carbon Nanofibers

Functionalized carbon nanofibers (FCNFs) were synthesized by the following procedure. 240 mg carbon nanofibers were added to a mixture of 100 mL HNO_3 [2.4 M] and 100 mL H_2SO_4 [7.6 M] and sonicated for 10 min. The mixture was then refluxed for 3 h at 100°C. After filtering through 0.2 µm glass-fiber filter, the acid treated nanofibers were washed with deionized water until pH ~ 7. The resulting nanofibers were dried under vacuum for 12 h at 60°C [6].

2.3. Fabrication of RC/FCNF/PPy (blend) Films

RC/FCNF/PPy films were fabricated as follows. 0.31 g polypyrrole was dispersed in 20 mL DMAC (Dimethyl acetamide) by ultrasonication for 1 h to make the stock solution. 0.12 g FCNFs were then dispersed in 50 mL previously prepared regenerated cellulose (RC) solution [9]. From the stock solution, 5.5 mL solution was mixed with the FCNFs dispersed regenerated cellulose solution. The mixture was then sonicated for 5 hours for homogenization. After that, the mixture was poured on a glass petri dish to cast films. The films were left for 24 h in an ambient atmosphere to remove solvent. The films were then washed in a mixture of deionized water and isopropyl alcohol of ratio 40:60 for 24 h. Finally, the films were soaked in DI water for 1 h and dried in air.

2.4. Fabrication of RC/FCNF/PPy (coated) Films

First, 0.21 g FCNFs were dispersed into 10 mL dimethylacetamide. The resulting solution was added to 20 mL previously prepared RC solution [9]. After ultrasonic dispersion (125 W) for 4 h, the RC/FCNF mixed solution (3.5 g in a 10 cm petri dish for each film) was poured on a glass petri dish. The solvent was evaporated and the films were dried in air. The films were then coated with polypyrrole by an adsorption-induced chemical polymerization technique. First, 9.3 g anthraquinone-2-sulfonic acid, sodium salt monohydrate, 5.34 g 5-sulfosalicylic acid dihydrate and 16.21 g ferric chloride hexahydrate ($FeCl_3.6H_2O$) were dissolved in 100 mL distilled water. 2.1 mL pyrrole was then dissolved in 100 mL distilled water and was poured into the above solution. FCNFs containing regenerated cellulose films were then immediately immersed in the polymerizing pyrrole solution for 40 min allowing in situ deposition of conductive polypyrrole on both sides of the films under ambient laboratory conditions. The films were then removed from the polymerizing solution, rinsed with distilled water, and dried in vacuum.

2.5. Electrical Property and Electromechanical Performance Measurement

To evaluate the presence of filler (FCNFs) and dopant on the properties of the composites, electrical conductivity of the composites was measured. Electrical conductivity of the films was determined by measuring surface resistance of the films at room conditions. The dimension of the samples was 2.5 cm X 0.7 cm X 45-50 µm. Electrical conductivity (σ_s) of the RC/FCNF/PPy matrices was calculated by the following equation:

$$\sigma_s = \frac{\Delta I}{\Delta V}\frac{l}{wd} \quad (1)$$

Where, l = length, w = width, d = thickness, and $\Delta I/\Delta V$ = the slope of the current versus voltage curve (Fig. 1). Prior to measurement, silver paste was painted (4 mm diameter) at the ends of the rectangular sample to ensure good electrical contact. The voltage was swept between 2-5 V and the resulting direct current was measured.

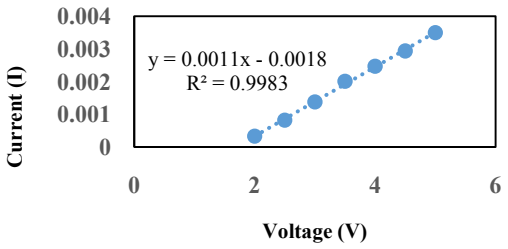

Figure 1. Current vs. Voltage curve for RC/FCNF/PPy (blend) film, y = Current (I), x = Voltage (V), R^2 = Correlation coefficient

The bending displacement was measured using a setup drawn in Fig. 2.

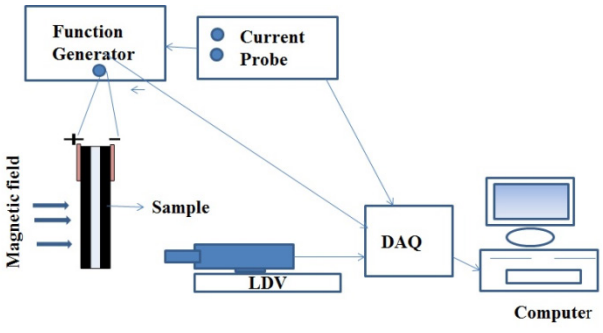

Figure 2. Bending displacement measurement setup

The setup consists of two laser displacement sensors (Keyence, LK-G85 and LK-G15), a current probe (Tektronix, TCP 300), a personal computer and a function generator (Agilent, 33220A). Copper electrodes attached to the samples worked to get good electrical contact with the function generator and the current probe. When an alternating current is applied to the film exposed to an external magnetic field, a Lorentz force was developed due to the interaction between an external magnetic field and an ac excitation current that deflects the free end of the film. This deflection is optically sensed by the laser displacement sensor. The reflected laser beam is collected using a position sensitive detector. The deflection of the films is increased, when the ac excitation current is applied with one frequency equal to the bending resonant frequency of the films. The deflection depends on the magnitude of the external magnetic field. Current probe measured the current passing through the sensor during actuation and the electrical power consumption was calculated thereby. The performance of the actuators at 90% relative humidity was evaluated to perform the actuation tests in an environmental chamber.

Scanning electron microscopy (SEM) images of the films were taken with a scanning electron microscope [Hitachi SU-70 FE SEM (field emission scanning electron microscope)] to study the microstructure of the films.

3. Results and Discussion

Generally, carboxyl groups are introduced on the surface of CNFs by functionalization. The groups on FCNFs can form hydrogen bonds with hydroxyl groups of cellulose (Fig. 3).

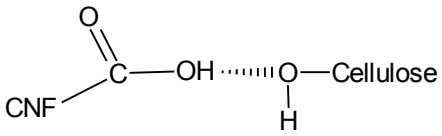

Figure 3. H-bonding between –OH group of cellulose and –COOH group of CNF

As a result, FCNFs can be dispersed in the layered structure of cellulose. Figure 4 shows FTIR spectra of carbon nanofibers (sample 1) and functionalized carbon nanofibers (sample 2). In sample 2, C=O stretch of carboxylic acid group appears from 1760-1690 cm^{-1} and O-H stretch appears at 3300 cm^{-1}.

RC/FCNF/PPy (coated) films showed electrical conductivity 0.54 S/cm. This value is seven orders of magnitude higher than pristine cellulose (8.22 X 10^{-8} S/cm at 50 percent relative humidity) [10]. This may be due to the presence of 2.0% FCNFs. It is clear that high electrical conductivity and high aspect ratio of FCNFs and their good dispersion (Fig. 5) in the composite help in achieving high electrical conductivity. In addition, the dopant has significant effect on the conductivity of the composite films.

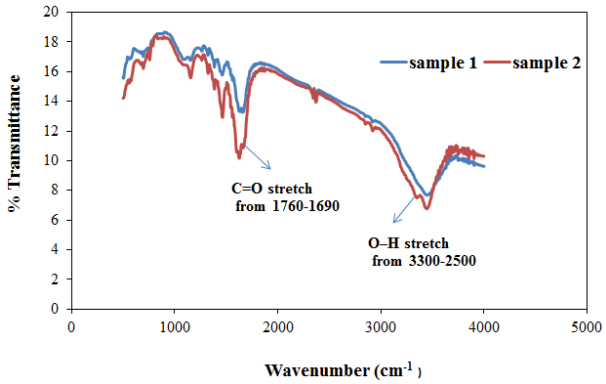

Figure 4. FTIR spectra of CNFs (sample 1) and FCNFs (sample 2)

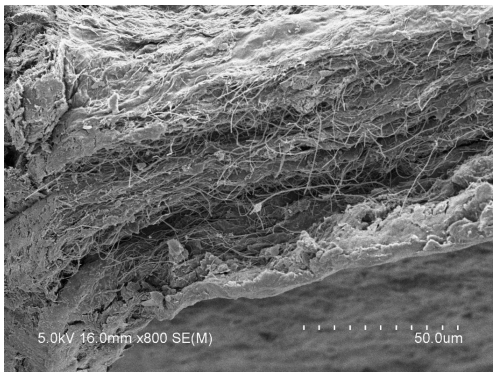

Figure 5. Cross-section image of RC/FCNF film

In this study, polypyrrole electrodes were deposited on both sides of the films by an in situ deposition technique using ferric chloride as an oxidant and anthraquinone-2-sulfonic acid sodium salt (AQSA-Na) as a dopant. AQSA-Na possesses an anthraquinone ring, and that gives good electrical conductivity of the composite films. RC/FCNF/PPy (coated) films show good electrical conductivity because of the presence of AQSA-Na as a dopant, along with suitable polymerization conditions. In addition, electrical conductivity of PPy depends on the conjugation length and inter-chain packing [11]. Moreover, PPy doped with AQSA-Na has a well-packed structure (Fig. 6) and the sulfonate may serve as a nucleus for PPy formation [12].

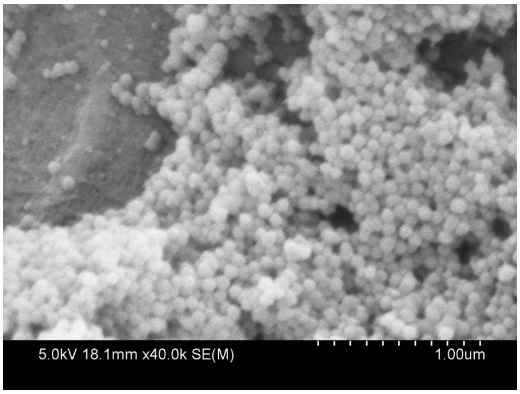

Figure 6. SEM image of PPyAQSA coated RC/FCNF film

RC/FCNF/PPy (blend) films show considerably lower electrical conductivity than the composites prepared by chemical deposition of PPy on RC/FCNF membrane. This is due to the mix-composite (blend) where the amount of PPy is below the critical volume for percolation, which results in a low conductivity value. In addition, the randomly distributed ball-like particles in the mix-composite (blend) have difficulties to form conductive paths (Fig. 7) [13].

Figure 7. Surface image of RC/FCNF/PPy (blend) film

In Figure 8 and 9, the absorption band at 1540-1560 cm^{-1} is due to the N-H bond, [14] and that confirms the presence of PPy in the RC/FCNF/PPy (blend) and the RC/FCNF/PPy (coated) films.

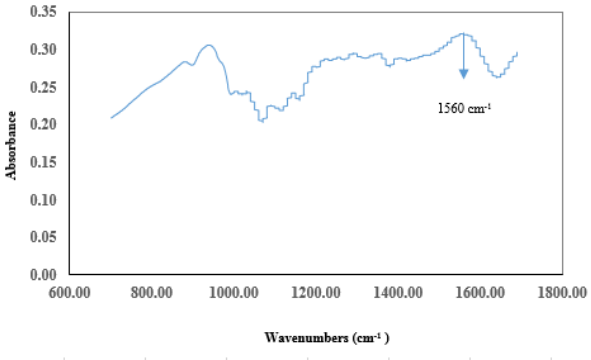

Figure 8. FTIR spectra of RC/FCNF/PPy (blend) film

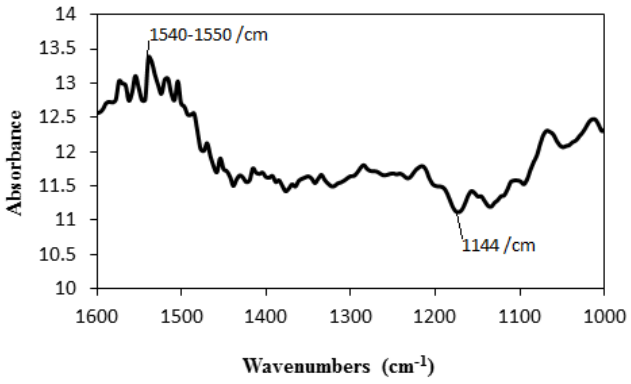

Figure 9. FTIR spectra of RC/FCNF/PPy (coated) film

Table below shows that the sensors developed in this study have better performance in terms of bending displacement because of higher electrical conductivity values compared to the RC/PPy/IL (coated) actuators developed by Suresha et al. [15] at 4.0 voltage.

Table 1. Displacement and Electrical Conductivity of the Actuators

Sample's Name	Thickness (µm)	Relative humidity (%)	Displacement (mm)	Electrical conductivity (S/cm) at 50% RH
RC/PPy /IL (Coated)	14-17	50	1.4	1.7 X 10^{-4} [15]
RC /FCNF /PPy (blend)	37-40	90 50	4.0 2.9	2.7 X 10^{-3}
RC /FCNF /PPy (Coated)	37-40	90 50	5.0 3.3	5.4 X 10^{-1}

RC/FCNF/PPy (coated) sensors showed higher bending displacement compared to the RC/FCNF/PPy (blend) sensors. RC/FCNF/PPy (coated) sensors have advantage of symmetry on both sides of the RC/FCNF. Both sides actuate the device more accurately as compared to the RC/FCNF/PPy (blend) sensors. RC/FCNF/PPy (coated) micro-sensor with the dimension of 1.6 cm X 0.8 cm X 40-45 µm detects magnetic fields about 6.4 µT, and has a resonance frequency of 7 Hz (Fig. 10), displacement of 3.3 mm and a power consumption of a few milliwatts at 50% RH. The sensors showed stable performance as AQSA-Na bearing an anthraquinone ring, which seemed to inhibit the reaction of PPy with oxygen. In addition, the sensors were attracted to magnets. This is due to the presence of large amount of defects in the graphene layers of the FCNFs. Further, magnetic moment and ferromagnetic interaction was enhanced by including H-atoms to zigzag edge in CNFs and a combination of vacancy defects and impurities (H, or N atoms from polypyrrole) [16].

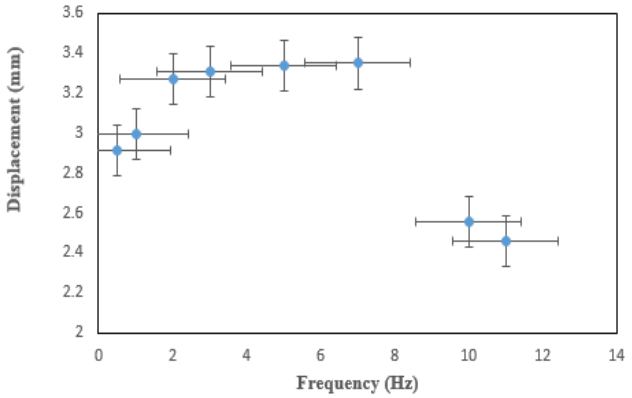

Figure 10. Displacement Vs Bending resonance frequency of the films

Electrical power consumption was measured during the

bending displacement test by measuring the current used. The RC/FCNF/PPy (coated) sensors consumed higher electrical power (0.19 mW cm^{-2}) compared to the RC/FCNF/PPy (blend) sensors (0.10 mW cm^{-2}) at 50% RH. The decreased power consumption is due to the decreased electrical conductivity of the RC/FCNF/PPy (blend) sensors. At 90% RH, the films retain some water, which resulted in increased ion mobility, which in turn improved the performance of the sensors (Table 1) but the power consumption was increased as electrical conductivity was increased. The power consumptions are below the microwave power limit for damaging living organs. This low power consumption is a promising factor for developing microwave driven sensors.

4. Conclusions

In this study, magnetic field sensors with resonant structures fabricated on MEMS technology has been presented. Lorentz-force based magnetic field sensors possess several specifications:

- Such as small size and ease of fabrication
- Low power consumption and high performance.
- Preparation process and dopants that have great impact on the electrical, electrochemical, mechanical and morphological properties of the sensors.
- The performance of the sensor depends on the RH around the sensors

Future applications of magnetic sensing ask for development of a multisensor on a single chip for measuring different parameters, including magnetic field, pressure, temperature, and acceleration is essential. However, MEMS technology needs to optimize the sensors operation for increasing resolution and life-time. [17].

ACKNOWLEDGEMENTS

The research was financially supported by the Institute of Biomedical Technologies, and technically supported by the School of Applied Sciences, Auckland University of Technology, New Zealand. The authors are grateful to Senior Research Officer Patrick Conor from faculty of Design & Creative Technologies for helping in taking SEM images.

REFERENCES

[1] Baschirotto, A., et al., Fluxgate magnetic sensor and front-end circuitry in an integrated microsystem. Sens. Actuators A, 2006. 132: p. 90-97.

[2] Diaz-Michelena, M., Small magnetic sensors for space applications. 2009. 9: p. 2271-2288.

[3] Perez, L., et al., Planar fluxgate sensor with an electrodeposited amorphous core. Sens. Actuators A, 2004. 109: p. 208-211.

[4] Jaehwan, K., Chun-Seok S., and Y. Sung-Ryul, Cellulose based electro-active papers: performance and environmental effects. Smart Mater. Struct, 2006. 15(3).

[5] Jaehwan, K., et al., Electro-active paper for a durable biomimetic actuator. Smart Mater. Struct., 2009. 18: p. 1-5.

[6] Sungryul, Y. and K. Jaehwan, Characteristics and performance of functionalized MWNT blended cellulose electro-active paper actuator. Synthetic Metals, 2008. 158: p. 521-526.

[7] Agustín, L.H., et al., Resonant Magnetic Field Sensors Based On MEMS Technology. Sensors, 2009: p. 7785-7813.

[8] Arnaud, M., et al., Cellular toxicity of carbon-based nanomaterials. Nano Lett., 2006. 6: p. 1121-1125.

[9] McCormick, C.L., A.C. Peter, and H.H.J. Brewer, Solution studies of cellulose in lithium chloride and N,N-dimethylacetamide. Macromolecules, 1985. 18(12): p. 2394–2401.

[10] Mahadeva, S.K. and J. K., Enhanced electrical properties of regenerated cellulose by polypyrrole and ionic liquid nanocoating. Journal of Nanoengineering and Nanosystems, 2011. 225(1): p. 33-39.

[11] Sage, B.H., in Encyclopedia of pharmaceutical Technology, J. Swarbrick and J.C. Boylan, Editors. 1993, Marcel Dekker Inc.:: New York. p. 217-247.

[12] Lin, R.Y., Y.C. Ou, and W.Y. Chen, The role of electroosmotic flow on in vitro transdermal iontophoresis. J. Control. Release., 1997. 43: p. 23-33.

[13] Li, C. and Z. Song, Diffusion-oxidative polymerization of transparent and conducting polypyrrole-poly(ethylene terephthalate) composites. Synth. Met., 1991. 40(1): p. 23-28.

[14] Rosner, R.B. and M.F. Rubner, Solid-state polymerization polypyrrole within a Langmuir-Blodgett film of ferric stearate. Chem. Mater, 1994. 6: p. 581–586.

[15] Suresha, K.M., & Jaehwan, K., Nanocoating of ionic liquid and polypyrrole for durable electro-active paper actuators working under ambient conditions. J. Phys. D: Appl. Phys., 2010 43(20): p. 5502.

[16] Zhang, Y., et al., First Principle studies of Defect Induced Magnetism in Carbon. Phys. Rev. Lett., 2007. 99.

[17] Yi, W.Q., et al., Improved Capacitive Performance of Polypyrrole Doped with 9,10 Anthraquinone sulfonic Acid SodiumSalt. Acta Phys. Chim. Sin., 2010. 26(11): p. 2951-2956.